

Variational Conditional-Dependence Hidden Markov Models for Human Action Recognition

Konstantinos P. Panousis ^{*1} Sotirios Chatzis ^{*2} Sergios Theodoridis ^{1,3}

Abstract

Hidden Markov Models (HMMs) are a powerful generative approach for modeling sequential data and time-series in general. However, the commonly employed assumption of the dependence of the current time frame to a single or multiple immediately preceding frames is unrealistic; more complicated dynamics potentially exist in real world scenarios. Human Action Recognition constitutes such a scenario, and has attracted increased attention with the advent of low-cost 3D sensors. The naturally arising variations and complex temporal dependencies have established this task as a challenging problem in the community. This paper revisits conventional sequential modeling approaches, aiming to address the problem of capturing time-varying temporal dependency patterns. To this end, we propose a different formulation of HMMs, whereby the dependence on past frames is dynamically inferred from the data. Specifically, we introduce a hierarchical extension by postulating an additional latent variable layer; therein, the (time-varying) temporal dependence patterns are treated as latent variables over which inference is performed. We leverage solid arguments from the Variational Bayes framework and derive a tractable inference algorithm based on the forward-backward algorithm. As we experimentally show using benchmark datasets, our approach yields competitive recognition accuracy and can effectively handle data with missing values.

1. Introduction

Modeling sequential data, typically encountered in many real-world applications such as bioinformatics and computer vision, remains a fundamental task in the field of machine learning. In this paper, we focus on human action recognition, which poses one of the most challenging tasks in the computer vision community. Researchers have devoted significant effort to address this particular area (Weinland et al., 2011) and remarkable progress has been made with the popularization of action recognition through 3D data (Aggarwal & Xia, 2014). However, the significant spatial and temporal variations arising in the execution of an action, along with variations due to the capturing process, e.g., camera occlusion, leave room for needed improvements in existing approaches.

Hidden Markov Models have been a popular approach for modeling sequential data, but more recently, have largely been replaced by their “deep” variants such as LSTMs and RNNs. Moreover, feedforward and convolutional neural networks have provided excellent results in many computer vision related tasks, i.e. image segmentation, classification, etc. Despite their success, these approaches exhibit significant drawbacks such as overparameterization even in simple tasks as image classification (Panousis et al., 2019), overfitting tendencies and lack of interpretability. On the other hand, HMMs offer a principled mathematical approach and flexibility to model complex sequential data accompanied by the explainability of generative approaches.

Several variants of Hidden Markov Models have been proposed in the literature aspiring to increase the potential of HMMs to deal with data characterized by spatial and temporal variations. For instance, a parametric distribution can be employed to cope with spatial variations and assist in the generalization of the model to unseen data (Wilson & Bobick, 1999). Hidden Semi Markov Models (HSMMs) (Yu, 2010) and their variants have been suggested for speed variations and more flexible temporal dynamics.

Recently, (Zhao et al., 2019) introduced a variant of a simple HSMM model, dubbed Hierarchical Dynamic Model (HDM). The proposed model is particularly tailored to deal with the spatial and temporal variations existent in the hu-

^{*}Equal contribution ¹Dept. of Informatics and Telecommunications, National and Kapodistrian University of Athens, Greece

²Dept. of Electrical Eng., Computer Eng., and Informatics, Cyprus University of Technology, Limassol, Cyprus ³The Chinese University of Hong Kong, Shenzhen, China.

man action recognition domain. Specifically, the considered hierarchical extension is performed by leveraging on the Bayesian framework to increase the capacity of the HSMMs to model human actions. The parameters of the model are allowed to vary as random variables and the flexibility of the model is further increased by utilizing algorithms for hyperparameter estimation. By relying on the Bayesian framework, the produced generative model is shown to be more robust to the natural variations of the data, exhibiting increased generalization capabilities, while at the same time requiring less data to train.

In contrast, first order HMMs are usually considered for simplicity and low computational complexity; the model's temporal dynamics are restrained to a simple step back, essentially undermining model effectiveness. This compromise is especially crucial in many applications where longer temporal dynamics may be present. Researchers have considered alternatives to alleviate this restriction, for example by introducing extended temporal dependencies in the form of second or higher order Markovian dynamics and had successful applications in many domains (Mari et al., 1994; Aycard et al., 2005; Nel et al., 2005; Engelbrecht & du Preez, 2010). However, the increased order introduces two significant drawbacks: (i) additional complexity to the model that may render it unusable in real-world scenarios and (ii) unnecessary burden to the researchers, namely the need to determine the best postulated order for each specific application and dataset. This strenuous process may additionally lead to unnecessary complex and overfitting models, negating the benefits and flexibility of HMMs. Lastly, a further drawback of conventional HMM approaches is the static and homogeneous assumptions (Begleiter et al., 2004; Chatzis, 2013; Chatzis et al., 2016), where the possible dynamic temporal dependencies of the data are ignored. The same effect applies to HSMMs; even though the relaxed temporal assumption allow for more flexible modeling of the dynamics, they still ignore potential non-homogeneous temporal dynamics in the data.

Drawing inspiration from these results, researchers have developed HMMs with variable order Markov chains, e.g., (Bhlmann & Wyner, 1999). The resulting models have been shown to be effective in a diverse range of applications, nevertheless exhibiting significant drawbacks such as the inability to model continuous observations (Dimitrakakis, 2010).

This paper draws from these results and attempts to offer a principled way of modeling sequential data with complex dynamics, such as the human action recognition task. To this end, we employ a variant of rigid HMMs that is able to capture complex temporal dependencies. The considered approach constitutes an hierarchical extension; by postulating an *additional latent first-order Markov Chain*,

called the *dependence-generator* layer, the model can alter the effective temporal dynamics of the conventional *observation-emitting* Markov Chain. In this way, the proposed approach can effectively infer which past state more strongly affects the current time frame. The proposed inferential construction for the considered model is enhanced by a fully Bayesian treatment under the Variational Inference framework. We posit that the considered hierarchical extension, when combined with the flexibility and effectiveness of *Variational Bayes*, can greatly increase the capacity of the resulting architecture to model sequential data that exhibit a complex combination of spatial and temporal variations.

We formulate efficient training and inference algorithms for our approach by: (i) deriving a variant of the classical forward-backward algorithm used in HMMs, (ii) relying on Variational Inference and conjugate priors for closed-form solutions. We dub our approach *Variational Bayesian Conditional Dependence Hidden Markov Model* (VB-CD-HMM) and evaluate its performance using well-known benchmark datasets for human action recognition. The provided empirical evidence vouches for the increased efficacy of the model to yield competitive predictive accuracy, consistent even in the presence of missing values.

The remainder of the paper is organized as follows: In Section 2, we present the proposed approach and the training and inference algorithms. The experimental results are presented in Section 3 along with some insights concerning the functionality and behavior of the temporal dynamics of the model. Finally, in Section 4, we summarize the contributions of our approach and present some directions for future research.

2. Proposed Model

In this work, we consider an extension of a conventional first order HMM, whereby an hierarchical structure is employed consisting of *two layers*: (i) a *dependence-generator* layer that comprises a simple first order Markov Chain that determines the *steps-back* taking place in the second layer and (ii) a chain of *observation-emitting* hidden states, where the temporal dependencies are determined from the output of the *dependence-generator* layer. To ensure tractability of the model's procedures, the *temporal dependencies* are *inferred* in a data-driven fashion. An outline of the envisaged Conditional Dependence-HMM (CD-HMM) model is provided in Fig. 1.

2.1. Model Definition

Let $Y = \{y_t\}_{t=1}^T \in \mathbb{R}^D$ be an observed data sequence with T time frames and D features. Following the definition of conventional HMMs, let us assume an N -state *emitting state sequence* denoted as $X = \{x_t\}_{t=1}^T, x_t \in [1, \dots, N]$

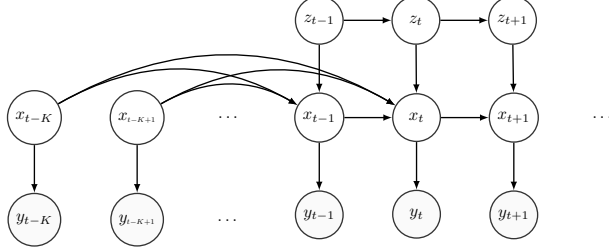


Figure 1. A graphical illustration of the considered Conditional Dependence Hidden Markov Model.

where x_t indicates the state from which the t^{th} observation is emitted. Each emission density is modeled by an M -component finite mixture model; the *mixture component indicators* are denoted as $L = \{l_t\}_{t=1}^T, l_t \in [1, \dots, M]$ with l_t indicating which mixture component generated the t^{th} observation.

The hierarchical construction postulates an additional layer, the *dependence-generator* layer, such that the *latent data* associated with each sequence are augmented by the supplementary sequence of *temporal dependence indicators*, $Z = \{z_t\}_{t=1}^T, z_t \in [1, \dots, K]$; indicators denoting the current temporal dependencies between the *observation-emitting* states at time t and times $t-1, \dots, t-K$ as shown in Fig. 1. Thus, different pairwise states (x_t, x_{t-z_t}) are considered for time t according to the value dictated by z_t .

The model parameters comprise $\theta = \{\phi, \psi\}$, where ϕ contains the parameters of the emission distributions of the model and ψ the effective parameters of the latent processes.

For the emission distributions, finite mixture models of multivariate Gaussian distributions are considered, such that

$$p(\mathbf{y}_t | x_t = i) = \sum_{m=1}^M c_{im} \mathcal{N}(\mathbf{y}_t | \boldsymbol{\mu}_{im}, R_{im}), \quad \forall i \quad (1)$$

where $\mathcal{N}(\cdot | \boldsymbol{\mu}, R)$ is a multivariate Normal distribution with mean $\boldsymbol{\mu} \in \mathbb{R}^D$ and precision matrix $R \in \mathbb{R}^{D \times D}$ with distinct parameters for each state and mixture; $c_i \in \mathbb{R}^M$ are the mixture component coefficients for state $x_t = i$. Hence, the effective parameters for the model distributions are $\phi = \{\boldsymbol{\mu}_{im}, R_{im}, c_{im}\}_{i,m=1}^{N,M}$.

Having defined the emission parameters of the model, we proceed with the definition of the parameters and their relationships pertaining to the postulated latent processes. Specifically, the first *dependence-generator* layer is a simple first order Markov Chain and is described by the following initial and transition probabilities:

$$\hat{\pi}_k \triangleq p(z_1 = k), \quad \forall k \quad (2)$$

$$\hat{A}_{kk'} \triangleq p(z_t = k' | z_{t-1} = k), \quad \forall t > 1, k, k' \quad (3)$$

For the second *observation-emitting* layer process, the initial

probability of the emitting state reads:

$$\pi_i \triangleq p(x_1 = i), \quad \forall i \quad (4)$$

To model the dependency between the first and second layers, and specifically for the second layer process, we define the set of *conditional dependence* transition probability matrices $\{A^k\}_{k=1}^K$, where $A^k \triangleq [A_{ij}^k]_{i,j=1}^N$, yielding:

$$\begin{aligned} A_{ij}^k &\triangleq p(x_t = j | x_{t-1}, \dots, x_{t-z_t}, z_t = k) \\ &= p(x_t = j | x_{t-k} = i, z_t = k) \end{aligned} \quad (5)$$

Thus, based on the inferred dependence of the first *dependence-generator* layer, we consider different temporal dependencies in the second layer. Intuitively, the conditional dependence determines the strength of the dependence to individual *past states*, altering the transition probability for the current *observation-emitting* state.

Having fully defined the parameters for the latent processes, the corresponding set comprises $\psi = \{\hat{\pi}, \hat{A}, \pi, \{A^k\}_{k=1}^K\}$. The definition of the model is now concluded.

The joint distribution reads:

$$p(Y, X, Z) = \hat{\pi}_{z_1} \pi_{x_1} \prod_{t=1}^{T-1} \hat{A}_{z_t, z_{t+1}} \prod_{t>1} A_{x_{t-z_t}, x_t}^z \prod_{t=1}^T p(\mathbf{y}_t | x_t)$$

2.2. Model Training

In this work, we employ arguments from the Bayesian framework to extend the CD-HMM model presented in the previous section using a *variational approximation*.

The *Variational Bayes* (VB) approach was chosen over Monte Carlo inference methods, e.g., Gibbs Sampling, considering the negligible performance differences and the significantly lower computational complexity.

The VB treatment of the model comprises the introduction of sets of appropriate prior distributions over all model parameters and maximization of the resulting Evidence Lower Bound (ELBO) expression. In order to obtain closed-form solutions for the updates of the parameters, we employ conjugate priors; a choice accompanied by the benefits of lower computational complexity and interpretability (Bishop, 2006; Chatzis, 2011; Theodoridis, 2015).

2.2.1. PRIORS AND EVIDENCE LOWER BOUND

Dirichlet distributions are imposed as the priors of the initial state probabilities for both layer processes $p(\pi) = \mathcal{D}(\pi | \boldsymbol{\eta}_0)$ and $p(\hat{\pi}) = \mathcal{D}(\hat{\pi} | \boldsymbol{\alpha}_0)$.

Analogous Dirichlet priors are imposed on the rows of the state transition probabilities and the mixture coefficients of the emission distributions.

For the prior over the means and precision matrices of the mixture components distributions for each hidden state and mixture, we assign a Normal-Wishart distribution with hyperparameters $\lambda_{ij}, \mathbf{m}_{ij}, \eta_{ij}, S_{ij}$ that reads

$$p(\boldsymbol{\mu}_{ij}, R_{ij}) = \mathcal{N}\mathcal{W}(\boldsymbol{\mu}_{ij}, R_{ij} | \lambda_{ij}, \mathbf{m}_{ij}, \eta_{ij}, S_{ij}), \forall i, j \quad (6)$$

This concludes the formulation of the prior specification for the VB-CD-HMM. A graphical illustration of the fully proposed model is shown in Fig. 2.

Exact inference of the marginal likelihood of the data is intractable for our model; nonetheless, employing the considered conjugate priors gives rise to an iterative procedure under the variational framework (Chatzis, 2011).

Let $\theta = \{\phi, \psi\}$ be the sets of latent processes' and emission distributions' parameters where a conjugate exponential prior has been imposed. In the VB treatment, we introduce an arbitrary distribution $q(\theta)$ and derive the Evidence Lower Bound (ELBO) for the model, a well-known lower bound on the marginal likelihood $p(Y)$, derived using Jensen's inequality (Jordan et al., 1999):

$$\log p(Y) \geq F(q) + \mathcal{KL}(q||p) \quad (7)$$

where $F(q) = \mathbb{E}_{q(\theta)} [p(Y, \theta)]$ and $\mathcal{KL}(q||p)$ is the *Kullback-Leibler* (KL) divergence, such that

$$\mathcal{KL}(q||p) = - \int d\theta q(\theta) \log \frac{q(\theta|Y)}{p(\theta)} \quad (8)$$

Maximizing the ELBO is equivalent to the minimization of the KL divergence between the true and the postulated posterior. We introduce the *mean-field* (posterior-independence) assumption on the joint variational posterior, such that $q(\theta)$ factorizes over all latent variables and model parameters.

Using equations (7) and (8), the ELBO can be written as

$$\begin{aligned} \text{ELBO} = & \mathbb{E}_{q(\theta)} \left[\log \left(\hat{\pi}_{z_1} \pi_{x_1} \prod_{t=1}^{T-1} \hat{A}_{z_t, z_{t+1}} \prod_{t>1}^T A_{x_t, x_{t-z_t}}^{z_t} \prod_{t=1}^T p(\mathbf{y}_t | \phi) \right) \right] \\ & + \mathbb{E}_{q(\theta)} \left[\log p(C, \pi, A, \hat{\pi}, \hat{A}, \boldsymbol{\mu}, \mathbf{R}) \right] - \mathbb{E}_{q(\theta)} [\log q(\theta)] \end{aligned} \quad (9)$$

Analytical expressions for the involved terms of Eq. (9) are provided in the supplementary material.

2.2.2. VARIATIONAL POSTERIORS

For each variable, the optimal member of the exponential family¹ can be found by maximizing (9). This maximization is performed in an EM-like fashion; in the E-step the parameters of the posterior distributions of the latent processes are updated, while in the M-step the rest of the variational distributions; the resulting iterative procedure is guaranteed to monotonically increase the ELBO.

¹Considering conjugate priors, the posteriors are expected to be of the same functional form as their corresponding priors.

2.2.3. M-STEP

We begin with the M-step of the algorithm, where we update the posteriors with respect to the parameters.

Starting from Eq.(9), we collect all relevant terms pertaining to the transition matrix of the first layer process \hat{A} ; we then maximize the resulting expression, yielding the following variational posterior:

$$q(\hat{A}) = \prod_{i=1}^K \text{Dir}(\hat{A}_{i1}, \dots, \hat{A}_{iK} | \omega_{i1}^{\hat{A}}, \dots, \omega_{iK}^{\hat{A}}) \quad (10)$$

where $\omega_{ij}^{\hat{A}} = \alpha_{ij} + \sum_t \gamma_{ijt}^{\hat{A}}$ and $\gamma_{ijt}^{\hat{A}} \triangleq q(z_t = i, z_{t-1} = j)$.

We follow the same procedure for the initial state probabilities $\hat{\pi}$, yielding:

$$q(\hat{\pi}) = \text{Dir}(\hat{\pi}_1, \dots, \hat{\pi}_K | \omega_1^{\hat{\pi}}, \dots, \omega_K^{\hat{\pi}}) \quad (11)$$

where $\omega_i^{\hat{\pi}} = \alpha_0^i + \gamma_i^{\hat{\pi}}$, and $\gamma_i^{\hat{\pi}} \triangleq q(z_1 = i)$.

The corresponding posteriors for the second layer process' parameters π read:

$$q(\pi) = \text{Dir}(\pi_1, \dots, \pi_N | \omega_1^\pi, \dots, \omega_N^\pi) \quad (12)$$

where $\omega_i^\pi = \eta_i^i + \gamma_i^\pi$ and $\gamma_i^\pi \triangleq q(x_1 = i)$.

And analogously for $A = \{A^k\}_{k=1}^K$:

$$q(A) = \prod_{k=1}^K \prod_{i=1}^N \text{Dir}(A_{i1}^k, \dots, A_{iN}^k | (\omega_{i1}^k)^A, \dots, (\omega_{iN}^k)^A) \quad (13)$$

with $(\omega_{ij}^k)^A = \eta_{ij}^k + (\gamma_{ij}^k)^A$ and $(\gamma_{ij}^k)^A = \sum_t q(x_t = i, x_{t+k} = j | z_t)$.

The corresponding expressions for the parameters and component coefficients of the emission distributions are derived analogously; analytical computations can be found in the supplementary material.

2.2.4. E-STEP

Turning to the E-step of the iterative procedure, the joint variational posterior optimizer for the latent processes Z and X , and the mixture component indicators L (and using Eq. (9)) reads:

$$q(Z, X, L) = \frac{\rho}{\sum_{Z, X, L} \rho} \quad (14)$$

where

$$\rho = \hat{\pi}_{z_1}^* \pi_{x_1}^* \prod_{t=1}^{T-1} \hat{A}_{z_t, z_{t+1}}^* \prod_{t=1}^T A_{x_t, x_{t-z_t}}^{*z_t} \prod_{t=1}^T c_{x_t l_t}^* p^*(\mathbf{y}_t | \phi_{x_t l_t}) \quad (15)$$

and

$$\hat{\pi}_i^* \triangleq \exp(\mathbb{E}_{q(\hat{\pi})}[\log \hat{\pi}_i]) \quad (16)$$

$$\pi_i^* \triangleq \exp(\mathbb{E}_{q(\pi)}[\log \pi_i]) \quad (17)$$

$$\hat{A}_{ij}^* \triangleq \exp(\mathbb{E}_{q(\hat{A})}[\log \hat{A}_{ij}]) \quad (18)$$

$$A_{ij}^{*k} \triangleq \exp(\mathbb{E}_{q(A)}[\log A_{ij}^k]) \quad (19)$$

$$c_{ij}^* \triangleq \exp(\mathbb{E}_{q(C)}[\log c_{ij}]) \quad (20)$$

$$p^*(\mathbf{y}_t | \theta_{x_t l_t}) \triangleq \exp(\mathbb{E}_{q(\phi)}[\log p(\mathbf{y}_t | \phi_{x_t l_t})]) \quad (21)$$

The variational posterior distribution defined in Eq. (14) is analogous to the expression of the conditional probability defined in the context of the conventional EM approach, where essentially (Chatzis, 2011),

$$q(Z, X, L) = p(Z, X, L | Y, \theta^*) \quad (22)$$

Thus, the variational posterior entails the calculation of the corresponding responsibilities that comprise said variational posterior $q(z_1 = i)$, $q(x_1 = 1)$, $q(z_t = i, z_{t-1} = j)$ and $q(x_t = j, x_{t-k} = i)$; these can easily be computed by means of the well-known forward backward algorithm. To this end, in the following, we derive a variant of the forward-backward algorithm for our model. We can then use the set of posterior expected values defined in Eqs. (16)-(21) as the current point estimates.

2.2.5. FORWARD-BACKWARD VARIANT

For calculating the forward-backward algorithm, we first define the forward messages as:

$$\alpha_t(\{x_\tau\}_{\tau=t-K+1}^t, z_t) \triangleq p(\{\mathbf{y}_\tau\}_{\tau=1}^t, \{x_\tau\}_{\tau=t-K+1}^t, z_t) \quad (23)$$

The defined messages can be computed recursively, using the following initialization:

$$\alpha_1(x_1, z_1) = \begin{cases} p(x_1 = i)p(\mathbf{y}_1 | x_1 = i), & z_1 = 1 \\ 0, & z_1 > 1 \end{cases} \quad (24)$$

and the induction step reads:

$$\alpha_t(\{x_\tau\}_{\tau=t-K+1}^t, z_t) = p(\mathbf{y}_t | x_t) \sum_{x_{t-K}} \sum_{z_{t-1}} p(z_t | z_{t-1}) \times p(x_t | x_{t-k}, z_t) \alpha_{t-1}(\{x_\tau\}_{\tau=t-K}^{t-1}, z_{t-1}) \quad (25)$$

The backward messages are analogously defined as:

$$\beta_t(\{x_\tau\}_{\tau=t-K+1}^t, z_t) \triangleq p(\{\mathbf{y}_\tau\}_{\tau=1}^t | \{x_\tau\}_{\tau=t-K+1}^t, z_t) \quad (26)$$

The corresponding initialization:

$$\beta_T(\{x_\tau\}_{\tau=t-K+1}^T, z_T = k) = 1, \quad \forall k \quad (27)$$

and recursion:

$$\begin{aligned} \beta_t(\{x_\tau\}_{\tau=t-K+1}^T, z_t) &= \sum_{x_{t+1}} \sum_{z_{t+1}} p(z_{t+1} | z_t) p(\mathbf{y}_{t+1} | x_{t+1}) \times \\ &p(x_{t+1} | x_{t-k+1}, z_{t+1}) \beta_{t+1}(\{x_\tau\}_{\tau=t-K+2}^T, z_{t+1}) \end{aligned} \quad (28)$$

2.2.6. RESPONSIBILITIES

By utilizing the forward-backward messages, the necessary responsibilities for updating the parameters of the model can now be computed.

For the first layer process, the marginal initial state responsibilities yield:

$$\begin{aligned} \gamma_t^z(k) &\triangleq p(z_t = k | \{\mathbf{y}_\tau\}_{\tau=1}^T) \propto \\ &\sum_X \alpha_t(\{x_\tau\}_{\tau=t-K+1}^t, z_t) \beta_t(\{x_\tau\}_{\tau=t-K+1}^t, z_t) \end{aligned} \quad (29)$$

Analogously, for the *observation-emitting* states:

$$\begin{aligned} \gamma_t^x(i) &\triangleq p(x_t = i | \{\mathbf{y}_\tau\}_{\tau=1}^T) \propto \\ &\sum_{X', z_t} \alpha_t(\{x_\tau\}_{\tau=t-K+1}^t, z_t) \beta_t(\{x_\tau\}_{\tau=t-K+1}^t, z_t) \end{aligned} \quad (30)$$

where $X' = \{x_\tau\}_{\tau=t-K+1}^t \setminus \{x_t\} = \{x_\tau\}_{\tau=t-K+1}^{t-1}$.

The state transitions responsibilities for the *temporal dependence* indicators read:

$$\begin{aligned} \gamma_t^z(k, k') &\triangleq p(z_t = k', z_{t-1} = k | \{\mathbf{y}_\tau\}_{\tau=1}^T) \propto \\ &\sum_{X'} \alpha_{t-1}(\{x_\tau\}_{\tau=t-K}^{t-1}, z_{t-1}) p(z_t | z_{t-1}) \times \\ &p(x_t | x_{t-k}, z_t) p(\mathbf{y}_t | x_t) \beta_t(\{x_\tau\}_{\tau=t-K}^t, z_t) \end{aligned} \quad (31)$$

Finally, the dependent state transition responsibilities:

$$\begin{aligned} \gamma_t^x(i, j, k) &\triangleq p(x_t = j, x_{t-k} = i | \{\mathbf{y}_\tau\}_{\tau=1}^T) \propto \\ &\sum_{X'', z_t} \alpha_t(\{x_\tau\}_{\tau=t-K+1}^t, z_t) \beta_t(\{x_\tau\}_{\tau=t-K+1}^t, z_t) \end{aligned} \quad (32)$$

where $X'' = \{x_\tau\}_{\tau=t-K+1}^t \setminus \{x_t, x_{t-k}\}$.

2.3. Inference

A common inference problem and one that is of great significance to the considered application is that of performing density estimation on a given test sequence with respect to a trained model. In the conventional HMM approaches, one can resort to the forward algorithm; we thus use the introduced variant for computing the predictive density.

Specifically for a simple CD-HMM trained model with parameters estimate $\hat{\theta}$, the density of a given test sequence

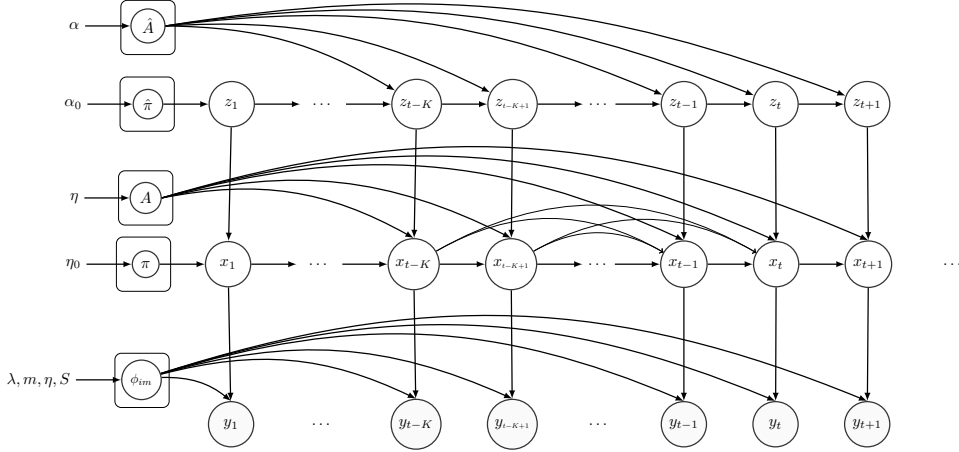


Figure 2. The resulting hierarchical model VB-CD-HMM after imposing appropriate conjugate prior distributions for all model parameters.

$Y^{\text{test}} = \{y_t^{\text{test}}\}_{t=1}^T$ yields:

$$p(Y^{\text{test}}|\hat{\theta}) = \sum_{z_T} \sum_X \alpha_T(x_{T-K+1}, \dots, x_T, z_T) \quad (33)$$

Now let us consider a VB-CD-HMM model, fully trained under the VB treatment using the training sequence Y . We need to calculate the predictive density of the test data:

$$p(Y^{\text{test}}|Y) = \int d\hat{\theta} p(\hat{\theta}|Y) P(Y^{\text{test}}|\hat{\theta}) \quad (34)$$

Using the introduced variational posterior in place of the unknown posterior $q(\hat{\theta}|Y)$, it can be shown (Chatzis, 2011):

$$\log q(Y^{\text{test}}|Y) \approx \text{Pred}(Y^{\text{test}}) \quad (35)$$

and

$$\text{Pred}(Y^{\text{test}}) = \sum_{Z, X, L} q(Z, X, L) \log \frac{\rho}{q(Z, X, L)} \quad (36)$$

Thus, we employ the forward variant defined in Section 2.2.5 utilizing the posterior expected values of the learned parameters $\hat{\theta}$. We can now classify test sequences according to their predictive density. Specifically, we train a different model for each action; an action label y^* is then assigned to a test sequence using the criterion $y_* = \text{argmax}_i \text{Pred}(Y^{\text{test}}|\hat{\theta}_i)$; $\hat{\theta}_i$ denotes the learned parameters for each different action.

3. Experimental Evaluation

In the following, we evaluate and compare our VB-CD-HMM approach on action recognition benchmarks. We assess the recognition accuracy of our model using the individual datasets and test the efficacy of our approach to data with missing values. We additionally present some further insights concerning the model complexity and behavior of the first layer process.

3.1. Parameter & Hyperparameter Selection

The resulting ELBO expression is non-convex with respect to the variational posterior, and potentially many local maxima exist; the obtained solution is thus dependent on the initialization of the parameters of the model. To avoid the rather time-consuming procedure of multiple runs from different initial values, we employ a common initialization scheme; KMeans is used to initialize the posterior parameters of the second layer process and the distributions' parameters. The parameters of the first postulated layer are initialized to random values, while for the hyperparameters we instead use *ad hoc* uninformative values, similar to (Chatzis, 2011).

3.2. Experimental Details

For our experimental evaluation we use four benchmark datasets for the human action recognition task, namely *MSR Action 3D (MSRA)* (Li et al., 2010), *UTD-MHAD (UTD)* (Chen et al., 2015), *Gaming 3D (G3D)* (Bloom et al., 2012) and *UPenn Action (Penn)* (Zhang et al., 2013). Only skeletal data are used for training the models. The preprocessing and augmentation of the data are the same as in (Zhao et al., 2019). We extract the motion of the joints for every pair of joints between two consecutive frames. PCA is then employed for dimensionality reduction, separately for joint positions and motions.

3.3. States, Mixtures and Temporal Dependencies

We trained different models with varying number of states and mixtures to investigate their effect on model effectiveness. In Fig. 3, a graphical representation of this effect is presented on the UTD dataset. As we observe, the recognition accuracy is not considerably sensitive to the chosen configuration; we run multiple configurations and retain the

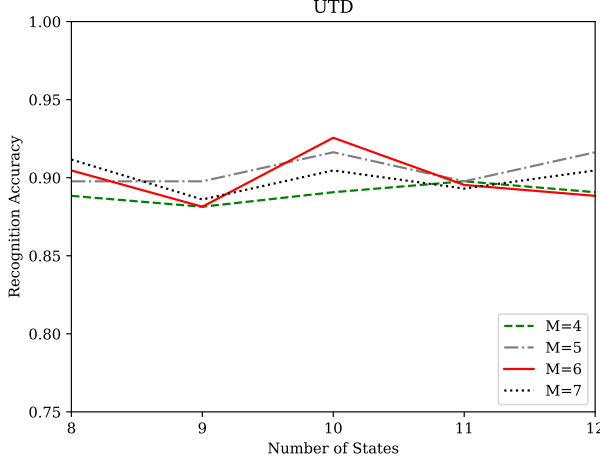


Figure 3. Recognition accuracy with respect to the number of states and number of mixtures used for the UTD dataset.

one with the higher ELBO.

For all experiments, we set $K = 2$, as we observed that the inferred temporal dependence posteriors rarely assigned high probability (if any) to $p(z_t > 2 | z_{t-1})$; this behavior is instinctive considering the characteristics of the considered features.

3.4. Experimental Results

We follow the train and test splits as suggested by the authors of the respective datasets. We compare our approach to similar benchmark adaptations of the base models along with a comparison with the HDM implementation (Zhao et al., 2019) using their PI, PL and BV variant; in the latter variational inference is utilized for the predictive likelihood. Their BG variant is based on Gibbs Sampling and is omitted from the following individual datasets results due to the dissimilarity and increased computational complexity relative to our approach. We further explore the performance differences when compared to other state-of-the arts methods.

3.4.1. INDIVIDUAL DATASETS

We first consider the MRSAs dataset, where the recognition rates of our approach can be found in the first column of Table 1. Compared to baseline models such as HMMs, HSMMs and LSTMs our model completely outperforms them in classification accuracy with an average improvement of 12.9%. HDM (Zhao et al., 2019), explicitly models spatial and temporal variations via an hierarchical HSMM; the parameters are allowed to vary as random variables. Even though HDM consistently improves over the considered alternatives, it falls short compared to the proposed VB-CD-HMM model. This behavior is consistent across all the considered datasets, resulting in an average classification accuracy of 89.45%, outperforming HDM by 1.45%. The

obtained empirical evidence suggest that our model benefits from the full Variational Bayesian approach, contrary to just using VB during inference. Additionally, the introduction of the additional *dependence generator* layer, can sufficiently cope with the temporal patterns of the data, without the need to resort to *Empirical Bayes* (Robbins, 1956).

We additionally compare the recognition accuracy of our approach to other state-of-the-art methods. The corresponding performances are illustrated in Table 3. As we observe, our approach yields clearly improved accuracy compared to the competition for UTD and Penn datasets. For the G3D dataset, our method slightly outperforms LRBM (Nie et al., 2015), but R3DG (Vemulapalli et al., 2014) performs better; that is due to the sophisticated feature engineering and combination of several approaches in contrast to our simple joints locations and motion features. Nevertheless, as we shall see in the next section, our method clearly outperforms R3DG, when we randomly omit observations; this behavior vouches for the improved robustness of our approach. Likewise, AL (Wang et al., 2012) considers a set of different features for the MSRA dataset, using more information, thus explaining the performance gap compared to our approach.

3.5. Missing Values

Generative models come with the additional benefit of robustness to missing values. This advantage is of great importance in the human action recognition field, especially when using skeletal data, where the dataset may be corrupted with missing observations, e.g., due to occlusion. As an HMM variant, the proposed CD-HMM model is such a generative model; we thus assess the efficacy of our approach when missing values are present. To this end, we train the considered architecture in the UTD, MSRA and G3D datasets, with randomly missing values from both the train and test data. Analogous experiments have been performed in (Zhao et al., 2019), and we adopt the same procedure, including the portion of missing values with respect to the original data. Thus, in Table 2, we report the recognition rates when we randomly omit 10%, 30% and 50% of the observations. As we observe, our method clearly outperforms the R3DG

Table 1. Recognition Accuracy (%) for individual dataset experiments using various benchmark models.

| Model | MSRA | UTD | G3D | Penn | Avg. |
|-----------|-------------|-------------|-------------|-------------|--------------|
| HMM | 67.8 | 82.8 | 68.1 | 82.3 | 75.3 |
| HSMM | 66.3 | 82.3 | 77.5 | 78.9 | 76.35 |
| LSTM | 74.7 | 77.0 | 82.2 | 90.3 | 81.1 |
| HCRF | 70.7 | 74.2 | 79.0 | 86.3 | 77.6 |
| HDM-PI | 70.3 | 84.4 | 79.4 | 89.8 | 81.0 |
| HDM-PL | 80.6 | 90.2 | 87.7 | 91.6 | 87.5 |
| HDM-BV | 82.1 | 91.4 | 87.7 | 90.8 | 88.0 |
| VB-CD-HMM | 82.5 | 92.7 | 90.6 | 92.0 | 89.45 |

Table 2. Recognition Accuracy (%) with missing values. Accuracies for R3DG (Vemulapalli et al., 2014), DLSTM (Zhu et al., 2016) and HDM (Zhao et al., 2019) were taken from the latter.

| Dataset | | UTD | | | MSRA | | | G3D | | |
|-----------------|---------------------------------|--------------|-------------|-------------|-------------|-------------|-------------|-------------|-------------|-------------|
| Missing Portion | | 10% | 30% | 50% | 10% | 30% | 50% | 10% | 30% | 50% |
| Model | R3DG (Vemulapalli et al., 2014) | 81.5 | 74.0 | 72.0 | 78.0 | 72.0 | 70.0 | 87.0 | 86.0 | 83.0 |
| | DLSTM (Zhu et al., 2016) | 70.5 | 66.0 | 63.0 | 68.0 | 63.0 | 61.0 | 81.0 | 76.0 | 73.0 |
| | HDM (Zhao et al., 2019) | 91.0 | 90.5 | 90.0 | 80.5 | 78.0 | 76.0 | 90.0 | 89.0 | 88.0 |
| | CD-HMM | 92.55 | 91.6 | 90.2 | 81.7 | 80.1 | 79.1 | 90.2 | 89.3 | 88.5 |

Table 3. Recognition accuracy for all the considered datasets compared to alternative methods.

| Dataset | Method | Acc. % |
|---------|---------------------------------|-------------|
| MSRA | AS(Ohn-Bar & Trivedi, 2013) | 83.5 |
| | AL(Wang et al., 2012) | 88.2 |
| | VB-CD-HMM | 82.5 |
| UTD | Fusion (Chen et al., 2015) | 79.1 |
| | DMM (Bulbul et al., 2015) | 84.1 |
| | CNN (Wang et al., 2016) | 85.8 |
| | VB-CD-HMM | 92.7 |
| G3D | LRBM (Nie et al., 2015) | 90.5 |
| | R3DG (Vemulapalli et al., 2014) | 91.1 |
| | VB-CD-HMM | 90.6 |
| Penn | Actemes(Zhang et al., 2013) | 86.5 |
| | AOG (Nie et al., 2015) | 84.8 |
| | VB-CD-HMM | 92.0 |

(Vemulapalli et al., 2014) and DLSTM (Zhu et al., 2016) methods by a clear margin. The same behavior is observed compared to the more relative HDM approach (Zhao et al., 2019). Note that even though the reported HDM accuracies are obtained through Gibbs sampling (BG variant) our approach exhibits the smallest decrease in recognition accuracy relative to the increase of missing values.

3.5.1. FURTHER INSIGHTS

We now turn to the memory complexity of CD-HMM. Assuming K temporal dependence states and N observation emitting states, a K -order and a simple HMM, the required number of parameters are presented in Table 4. We ad-

Table 4. Required number of parameters for HMM approaches. We assume the same number of emission parameters for all methods.

| Model | # Parameters |
|---------|--|
| HMM | $(N - 1) + N(N - 1)$ |
| HMM^K | $N^K(N - 1)$ |
| CD-HMM | $(K - 1) + K(K - 1) + (N - 1) + N(N - 1)K$ |

ditionally assess the training and inference times for VB-CD-HMM ($K = 2$) and for a first-order HMM. We run multiple experiments with the same configurations; training is 5% slower for VB-CD-HMM, while for inference the differences are negligible. Hence, in stark contrast to high order HMMs, VB-CD-HMM can effectively model complex

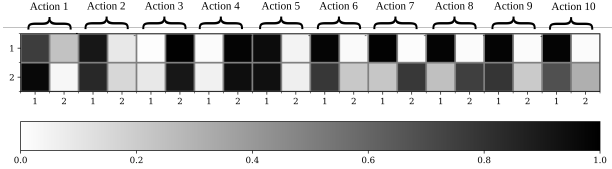


Figure 4. The inferred temporal dependence indicators $A_{kk'} = p(z_t = k'|z_{t-1} = k)$ for the first 10 actions in the UTD dataset. Black denotes very high probability, while white very low.

temporal patterns with a minor training overhead.

Finally, we examine the patterns of the first layer process, the *dependence generator* layer of an CD-HMM model, to gain further insights to the behavior of the model and assert that the temporal dependencies do not collapse to simple first order dynamics, reducing the model to a conventional HMM. To this end, we focus on a trained model on the *UTD* dataset and choose a subset of ten actions to investigate their posterior parameters concerning the generation of dependencies. As is clearly shown in Fig. 4, the distribution of temporal dependencies is essentially different for different actions, providing strong empirical evidence that the introduced mechanism can capture complex temporal variations in the data.

4. Conclusions

In this paper, we introduced a generative approach to the human action recognition task, where we employ a more expressive HMM model that allows for competitive recognition accuracies. To this end, we considered an hierarchical extension by postulating an additional layer process that can capture time-varying temporal dependencies; we augmented our model with a fully Variational Bayesian adaptation. Our experiments have provided strong empirical evidence of the efficacy of our approach. Note that the considered model: (i) provides *high recognition accuracies* for all the considered datasets, (ii) can effectively model data with missing observations while exhibiting the *smallest decrease* in accuracy and (iii) the postulated first layer process yields *distinct temporal dynamics* for different actions. In our future work, we intend to examine how a non-parametric approach can further increase the capacity of our approach.

References

Aggarwal, J. and Xia, L. Human activity recognition from 3d data: A review. *Pattern Recognition Letters*, 48, 10 2014.

Aycard, O., Mari, J., and Washington, R. Learning to automatically detect features for mobile robots using second-order hidden markov models. *Int J Adv Robotic Sy*, 1, 01 2005.

Begleiter, R., El-Yaniv, R., and Yona, G. On prediction using variable order markov models. *J. Artif. Int. Res.*, 22, December 2004.

Bishop, C. M. *PRML (Information Science and Statistics)*. Springer-Verlag, Berlin, Heidelberg, 2006.

Bloom, V., Makris, D., and Argyriou, V. G3d: A gaming action dataset and real time action recognition evaluation framework. In *2012 IEEE Computer Society Conference on Computer Vision and Pattern Recognition Workshops*, June 2012.

Bulbul, M. F., Jiang, Y., and Ma, J. Dmms-based multiple features fusion for human action recognition. *Int. J. Multimed. Data Eng. Manag.*, 6:2339, October 2015.

Bhlmann, P. and Wyner, A. J. Variable length markov chains. *Ann. Statist.*, 27, 04 1999.

Chatzis, S., Kosmopoulos, D., and Papadourakis, G. A nonstationary hidden markov model with approximately infinitely-long time-dependencies. *International Journal on Artificial Intelligence Tools*, 25, 2016.

Chatzis, S. P. A variational bayesian methodology for hidden markov models utilizing student's-t mixtures. *Pattern Recognition*, 44, 2011.

Chatzis, S. P. Margin-maximizing classification of sequential data with infinitely-long temporal dependencies. *Expert Systems with Applications*, 40, 2013.

Chen, C., Jafari, R., and Kehtarnavaz, N. Utd-mhad: A multimodal dataset for human action recognition utilizing a depth camera and a wearable inertial sensor. In *2015 IEEE International Conference on Image Processing (ICIP)*, Sep. 2015.

Dimitrakakis, C. Bayesian variable order markov models. In *Proceedings of the Thirteenth International Conference on Artificial Intelligence and Statistics*, volume 9 of *Proceedings of Machine Learning Research*. PMLR, 13–15 May 2010.

Engelbrecht, H. and du Preez, J. Efficient backward decoding of high-order hidden markov models. *Pattern Recognition*, 43, 2010.

Jordan, M. I., Ghahramani, Z., Jaakkola, T. S., and Saul, L. K. An introduction to variational methods for graphical models. *Mach. Learn.*, 37, November 1999.

Li, W., Zhang, Z., and Liu, Z. Action recognition based on a bag of 3d points. In *2010 IEEE Computer Society Conference on Computer Vision and Pattern Recognition - Workshops, CVPRW 2010*, 07 2010.

Mari, J.-F., Haton, J. P., and Kriouile, A. Automatic word recognition based on second-order hidden markov models. *IEEE Trans. Speech and Audio Processing*, 5, 1994.

Nel, E., du Preez, J. A., and Herbst, B. M. Estimating the pen trajectories of static signatures using hidden markov models. *IEEE Transactions on Pattern Analysis and Machine Intelligence*, 27, Nov. 2005.

Nie, B. X., Xiong, C., and Zhu, S. Joint action recognition and pose estimation from video. In *2015 IEEE Conference on Computer Vision and Pattern Recognition (CVPR)*, pp. 1293–1301, June 2015.

Nie, S., Wang, Z., and Ji, Q. A generative restricted boltzmann machine based method for high-dimensional motion data modeling. *Comput. Vis. Image Underst.*, 136: 1422, July 2015.

Ohn-Bar, E. and Trivedi, M. M. Joint angles similarities and hog2 for action recognition. In *2013 IEEE Conference on Computer Vision and Pattern Recognition Workshops*, pp. 465–470, June 2013.

Panousis, K., Chatzis, S., and Theodoridis, S. Nonparametric Bayesian deep networks with local competition. In *Proceedings of the 36th International Conference on Machine Learning*, volume 97 of *Procs of Machine Learning Research*. PMLR, Jun 2019.

Robbins, H. An empirical bayes approach to statistics. In *Proceedings of the Third Berkeley Symposium on Mathematical Statistics and Probability, Volume 1: Contributions to the Theory of Statistics*, Berkeley, Calif., 1956. University of California Press.

Theodoridis, S. *Machine Learning: A Bayesian and Optimization Perspective*. Academic Press, Inc., USA, 1st edition, 2015.

Vemulapalli, R., Arrate, F., and Chellappa, R. Human action recognition by representing 3d skeletons as points in a lie group. In *2014 IEEE Conference on Computer Vision and Pattern Recognition*, pp. 588–595, June 2014.

Wang, J., Liu, Z., Wu, Y., and Yuan, J. Mining actionlet ensemble for action recognition with depth cameras. IEEE International Conference on Computer Vision and Pattern Recognition (CVPR), June 2012.

Wang, P., Li, Z., Hou, Y., and Li, W. Action recognition based on joint trajectory maps using convolutional neural networks. In *Procs. ICM, MM 16*, pp. 102106, New York, NY, USA, 2016. Association for Computing Machinery.

Weinland, D., Ronfard, R., and Boyer, E. A survey of vision-based methods for action representation, segmentation and recognition. *Comput. Vis. Image Underst.*, 115, 2011.

Wilson, A. and Bobick, A. Parametric hidden markov models for gesture recognition. *Pattern Analysis and Machine Intelligence, IEEE Transactions on*, 21, 10 1999.

Yu, S.-Z. Hidden semi-markov models. *Artif. Intell.*, 174, 2010.

Zhang, W., Zhu, M., and Derpanis, K. G. From actemes to action: A strongly-supervised representation for detailed action understanding. In *The IEEE International Conference on Computer Vision (ICCV)*, Dec. 2013.

Zhao, R., Xu, W., Su, H., and Ji, Q. Bayesian hierarchical dynamic model for human action recognition. In *The IEEE Conference on Computer Vision and Pattern Recognition (CVPR)*, June 2019.

Zhu, W., Lan, C., Xing, J., Zeng, W., Li, Y., Shen, L., and Xie, X. Co-occurrence feature learning for skeleton based action recognition using regularized deep lstm networks. In *Proceedings of the Thirtieth AAAI Conference on Artificial Intelligence*, AAAI16, pp. 36973703. AAAI Press, 2016.